



CHORUS

This is the accepted manuscript made available via CHORUS. The article has been published as:

Multichannel Kondo Impurity Dynamics in a Majorana Device

A. Altland, B. Béri, R. Egger, and A. M. Tsvelik

Phys. Rev. Lett. **113**, 076401 — Published 11 August 2014

DOI: [10.1103/PhysRevLett.113.076401](https://doi.org/10.1103/PhysRevLett.113.076401)

Multi-channel Kondo impurity dynamics in a Majorana device

A. Altland,¹ B. Béri,² R. Egger,³ and A.M. Tsvelik⁴

¹*Institut für Theoretische Physik, Universität zu Köln, Zùlpicher Str. 77, D-50937 Köln, Germany*
²*School of Physics and Astronomy, University of Birmingham, Edgbaston, Birmingham B15 2TT, UK*

³*Institut für Theoretische Physik, Heinrich-Heine-Universität, D-40225 Düsseldorf, Germany*

⁴*Department of Condensed Matter Physics and Materials Science,
Brookhaven National Laboratory, Upton, NY 11973-5000, USA*

We study the multi-channel Kondo impurity dynamics realized in a mesoscopic superconducting island connected to metallic leads. The effective “impurity spin” is non-locally realized by Majorana bound states and strongly coupled to lead electrons by non-Fermi liquid correlations. We explore the spin dynamics and its observable ramifications near the low-temperature fixed point. The topological protection of the system raises the perspective to observe multi-channel Kondo impurity dynamics in experimentally realistic environments.

PACS numbers: 71.10.Pm, 73.23.-b, 74.50.+r

Introduction.—The coupling of a local quantum degree of freedom (“impurity”) to an ideal Fermi gas can generate strong correlations which ultimately may push the system outside the realm of the Fermi liquid. The best known realization of this phenomenon is the multi-channel Kondo effect in the overscreened regime $M > 2S$, where the impurity is a local spin- S degree of freedom and the Fermi gas is realized as a set of M one-dimensional conduction channels. The multi-channel Kondo effect has been the subject of a huge body of theoretical studies, and the non-perturbative mechanisms behind the formation of its non-Fermi liquid fixed points are by now well understood [1–7]. At the same time, the experimental realization of this seemingly rather basic system is met with severe difficulties [8], since anisotropies in the couplings between impurity and different channels are relevant perturbations [1]. As a consequence, a delicate fine tuning of coupling constants is required, a condition few if any realizations of the system are able to meet. For the same reason, the highly entangled effective degrees of freedom predicted to form at strong coupling [2–5] have so far remained beyond experimental access.

The recently proposed “topological” Kondo effect [9] promises a rather more robust realization of non-Fermi liquid correlations. In this system, schematically indicated in Fig. 1, the “impurity” is formed by the M_{tot} Majorana end states of spin-orbit coupled quantum wires in proximity to a finite piece of s -wave superconducting material [14–16] — a setup realizable by current device technology [18–23]. The mutual coupling h_{ij} between Majorana bound states $i, j = 1, \dots, M_{\text{tot}}$ is often significant and can be tuned by external gates; in the spin analogy, it plays the role of an effective Zeeman field. Tunnel coupling $M \leq M_{\text{tot}}$ Majoranas to normal leads, see Fig. 1, generates an effective Kondo setup, where the “reality” of the compound Majorana states implies that $\text{SO}(M)$ rather than the more conventional $\text{SU}(2)$ (but see Refs. [24, 25]) plays the role of the symmetry group. Importantly, the non-Fermi liquid Kondo fixed point of

such a device is self-stabilizing: Regardless of disparities in the lead-to-Majorana tunnel couplings or other sources of channel anisotropy, it will be approached at low temperatures. Signatures of this flow in, e.g., the power-law scaling of conductance coefficients have been the subject of Refs. [9, 11–13].

However, arguably the most striking manifestation of quantum criticality in the multi-channel Kondo effect is the formation of a massively entangled effective degree of freedom governing the system at strong coupling. In this Letter, we argue that mesoscopic Majorana devices offer, for the first time, a perspective to probe and manipulate such type of quantum degrees of freedom within a challenging yet realistic experimental setup. The readout observables in this context are various transport coefficients and “spin” expectation values, while the “knobs” to manipulate the non-Fermi liquid impurity are the Zeeman field coefficients mentioned above. Our main findings are summarized as follows: (i) We show that the Zeeman field strongly affects the conductance coefficients, G_{jk} , as well as the “magnetization”, i.e., the expectation value of the Majorana spin components. On intermediate temperature scales, both observables can be accessed by perturbation theory around the fixed point. We also propose a scheme to experimentally probe the magnetization in terms of a protocol involving a joint tuning of the Zeeman field and the tunnel couplings to the leads. (ii) We show that the Majorana spin has nonvanishing M -point ($M/2$ -point) correlation functions for odd (even) M , and how these imply the existence of nonlinear susceptibilities and frequency mixing. In the conventional two-channel $\text{SU}(2)$ Kondo model, such effects are absent. (iii) For very low temperatures, the Zeeman field destabilizes the Kondo fixed point. Specifically, a field with just one component drives a crossover between two Kondo fixed points with $M \rightarrow M - 2$, which will manifest itself in a definite change of, e.g., the temperature dependence of transport coefficients.

Generally speaking, the macroscopic realization of our

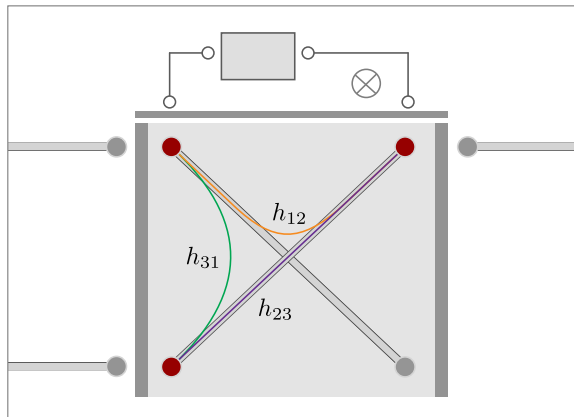


Figure 1. (Color online) Schematic setup leading to the topological Kondo effect. A floating superconducting island (center square) with charging energy E_c supports a helical crossed nanowire [10]; alternative realizations using several nanowires are also possible. At the terminal points of the wires, Majorana fermions γ_j (the circles) are present [14–16], M of which are coupled to external leads (here $M = 3$). Direct tunnel couplings h_{jk} between the Majoranas act like a Zeeman field on this “Majorana impurity spin”. The upper part illustrates the optional coupling to a single-electron box via flux-tunable tunnel amplitudes. This provides a way [17] to read out the effective “magnetization” $\sim i(\gamma_j\gamma_k)$.

“impurity” in terms of long-range entangled Majoranas should make the system more accessible than a “real” spin or other microscopic few-level systems. It is also worth pointing out that all phenomena listed above essentially rely on the “Zeeman” coefficients h_{ij} , i.e., on couplings generally considered obstructive to the observation of Majoranas. In the present context, the dependence of observables on these quantities is a defining element of the theory, and it stands to reason that the observation of any of the effects (i)-(iii) would provide compelling evidence for Majorana fermions.

Model.— We consider a setup as shown schematically in Fig. 1. The set of M Majorana fermions tunnel connected to leads is described by operators $\gamma_j = \gamma_j^\dagger$ subject to the Clifford algebra $\{\gamma_j, \gamma_k\} = 2\delta_{jk}$ [14–16]. The $\{\gamma_j\}$ compose a spinor representation of the $SO(M)$ group, and the $M(M-1)/2$ different products $i\gamma_j\gamma_k$ define the components of the Majorana spin. The Hamiltonian describing the system at energy scales below the island charging energy, E_c , is [9, 11–13]

$$H = -i \sum_{j=1}^M \int_{-\infty}^{\infty} dx \psi_j^\dagger(x) \partial_x \psi_j(x) \quad (1)$$

$$+ \sum_{j \neq k} \lambda_{jk} \gamma_j \gamma_k \psi_k^\dagger(0) \psi_j(0) + i \sum_{j \neq k} h_{jk} \gamma_j \gamma_k,$$

where $\psi_j(x)$ is an effectively spinless right-moving fermion field describing the j th lead; unfolding from

$x < 0$ to the full line is understood, with $x = 0$ at the tunnel contact. (We set the Fermi velocity $v = 1$ and use units with $\hbar = k_B = 1$.) The symmetric matrix of “exchange couplings” is given by $\lambda_{jk} \approx t_j t_k / E_c > 0$, with lead-Majorana tunnel couplings t_j , while the direct couplings $h_{jk} = -h_{kj}$ between Majoranas act like Zeeman fields. Concerning the remaining $M_{\text{tot}} - M$ Majoranas on the island which are not coupled to leads, we assume that these have no direct tunnel couplings with the γ_j [26]. For $h_{jk} = 0$ and on energy scales below the Kondo temperature

$$T_K \simeq E_c \exp\left(-\frac{\pi}{(M-2)\bar{\lambda}}\right), \quad (2)$$

with average exchange coupling $\bar{\lambda}$, the model (1) scales to the topological Kondo fixed point [9]. In contrast to conventional multi-channel Kondo systems [1–7, 27], anisotropy in the λ_{jk} is an irrelevant perturbation near the fixed point, which in turn corresponds to an $SO_2(M)$ Wess-Zumino-Novikov-Witten boundary conformal field theory (BCFT) [5, 28]. While the ensuing physics can be discussed within the framework of the Affleck-Ludwig [5] BCFT approach (adapted to the $SO_2(M)$ case), it also admits a more direct bosonization description.

Abelian bosonization.— In terms of bosonization, the lead Hamiltonian in Eq. (1) is represented as $H_{\text{lead}} = \frac{1}{8\pi} \sum_j \int dx [(\partial_x \theta_j)^2 + (\partial_x \varphi_j)^2]$, where θ_j and φ_j are dual bosonic fields [6, 29] defined for $x < 0$, with boundary condition $\varphi_j(0) = (\partial_x \theta_j)(0) = 0$ at the tunnel contact. In addition to the γ_j , the exchange coupling term in Eq. (1) involves the lead electron operators at $x = 0$, which are represented by $\psi_j(0) = \frac{i}{\sqrt{a}} \Gamma_j e^{i\theta_j(0)/2}$ [30, 31] with the short-distance length a . The Klein factors $\Gamma_j = \Gamma_j^\dagger$ establish anticommutation relations between electrons on different leads [29], $\{\Gamma_j, \Gamma_k\} = 2\delta_{jk}$ and $\{\Gamma_j, \gamma_k\} = 0$, and can be represented as auxiliary Majorana fermions [11–13]. Redefining $\lambda_{jk} \rightarrow a\lambda_{jk}$, the exchange term then becomes $H_K = \sum_{j \neq k} \lambda_{jk} \gamma_j \Gamma_j \gamma_k \Gamma_k e^{-i[\theta_k(0) - \theta_j(0)]/2}$.

Combining physical Majoranas and Klein factors to the “hybrid” fermion operators $d_j = (\gamma_j + i\Gamma_j)/2$, both types of Majorana fermions enter only through the products $p_j p_k$ of the parities of the hybrid fermions shared between them, $p_j = i\gamma_j \Gamma_j = 2d_j^\dagger d_j - 1 = \pm 1$. As parity products commute, they can be simultaneously diagonalized, $p_j p_k = \pm 1$. At first sight, the p_j themselves seem to generate good quantum numbers. However, the total fermion parity also has to be conserved, $P_{\text{tot}} \sim \prod_{j=1}^{M_{\text{tot}}} \gamma_j = \pm 1$. This parity constraint holds when no above-gap quasiparticles are accessible, and reflects the fixed total electron number on the island within the topological Kondo regime. Since $\{p_j, P_{\text{tot}}\} = 0$, the parity constraint is violated by individual p_j operators. Similar constraints on compound Majorana systems have been discussed recently [32–34], and must be taken into account on top of the Clifford algebra. Here

we have $M - 1$ independent conserved parity products, e.g., $p_j p_M = \pm 1$, such that we arrive at a purely bosonic problem for given collection $\{p_j p_k\}$.

Kondo fixed point.—For $h_{jk} = 0$, the renormalization group (RG) flow of the λ_{jk} proceeds towards an isotropic strong-coupling fixed point. The effect of this becomes transparent after an orthogonal rotation of the boson fields, $\boldsymbol{\theta} = (\theta_1, \dots, \theta_M)$ and $\boldsymbol{\varphi} = (\varphi_1, \dots, \varphi_M)$. Using the unit vector $\mathbf{v}_0 = \frac{1}{\sqrt{M}}(1, \dots, 1)$, we decompose them to $\theta_0 = \mathbf{v}_0 \cdot \boldsymbol{\theta}$ and $\varphi_0 = \mathbf{v}_0 \cdot \boldsymbol{\varphi}$, with the remaining $M - 1$ components $\tilde{\theta}_j$ and $\tilde{\varphi}_j$, respectively, along the directions orthogonal to \mathbf{v}_0 . This rotation decouples the (θ_0, φ_0) sector, and the exchange term becomes

$$H_K = - \sum_{j \neq k} \lambda_{jk} p_j p_k \exp \left(\frac{i}{2} (\mathbf{w}_k - \mathbf{w}_j) \cdot \tilde{\boldsymbol{\theta}}(0) \right). \quad (3)$$

The M vectors \mathbf{w}_j are of dimension $M - 1$, with $\mathbf{w}_j \cdot \mathbf{w}_l = \delta_{jl} - 1/M$, and span the field space orthogonal to the zero modes. For each set $\{p_j p_k\}$, Eq. (3) defines a boundary potential with minima forming a hyper-triangular lattice [30, 31, 35, 36]. Near the $\lambda_{jk} \rightarrow \infty$ fixed point, $\tilde{\boldsymbol{\theta}}(0)$ tends to be pinned to one of these $\{p_j p_k\}$ -dependent minima. The weak-coupling Neumann boundary conditions of $\boldsymbol{\theta}$ are thus dynamically replaced by Dirichlet conditions for $\tilde{\boldsymbol{\theta}}$ near the Kondo limit. For $h_{jk} = 0$, the leading perturbations are due to operators preserving $\{p_j p_k\}$ while tunneling $\tilde{\boldsymbol{\theta}}(0)$ between adjacent minima [11, 12]. These perturbations are RG irrelevant, of scaling dimension $\Delta_{\text{irr}} = 1 + \frac{M-2}{M} > 1$, consistent with a stable fixed point. Δ_{irr} also coincides with that of the first descendant of the adjoint primary, which we identify as the leading perturbation of the $\text{SO}_2(M)$ BCFT. Near this fixed point, the high-energy cutoff scale of the theory is then set by the Kondo temperature T_K in Eq. (2).

Majorana spin at strong coupling.—The Zeeman term generates RG relevant perturbations which destabilize the $\text{SO}(M)$ Kondo fixed point. In terms of symmetries, this is because the Zeeman field breaks an emergent time-reversal invariance of Eq. (1). In terms of bosonization, the reason is that $\gamma_j \gamma_k$ does not commute with all possible products $p_m p_n$. This implies that additional tunneling processes can take place, where $\tilde{\boldsymbol{\theta}}(0)$ connects minima belonging to different $\{p_j p_k\}$ sectors. For short enough tunneling “distance”, such a process becomes RG relevant. The corresponding scaling operator \mathcal{S}_{jk} conjugate to h_{jk} can be inferred from symmetry arguments. In particular, \mathcal{S}_{jk} should (i) conserve all $p_m p_n$ products commuting with $\gamma_j \gamma_k$, (ii) respect the $\tilde{\boldsymbol{\theta}}$ Dirichlet conditions, (iii) should have the same $\text{SO}(M)$ rotational properties as the Zeeman perturbation, (iv) commute with P_{tot} , (v) conserve charge, and (vi) be a local operator acting at the “impurity” position. Conditions (i) to (vi) determine [37] the bosonized representation of the Majorana spin near the Kondo fixed point: $\mathcal{S}_{jk} \sim \mathcal{S}_{jk}^{(+)} + \mathcal{S}_{jk}^{(-)}$ consists of the

“bare” operator dressed by bosonic phase factors,

$$\mathcal{S}_{jk}^{(\pm)} = i \gamma_j \gamma_k \cos \left(\frac{1}{2} (\mathbf{w}_j \pm \mathbf{w}_k) \cdot \tilde{\boldsymbol{\varphi}}(0) \right). \quad (4)$$

Depending on the sign, the operators in Eq. (4) have dimension $\Delta_+ = 1 - \frac{2}{M}$ (relevant) or $\Delta_- = 1$ (marginal), identical to those of the adjoint primary and the descendant of the identity, respectively. We have thus identified these operators as the leading time-reversal symmetry breaking perturbations of the $\text{SO}_2(M)$ BCFT. For small h_{jk} , it suffices to keep only the RG relevant operator in the Zeeman term. This still represents a weak perturbation around the Kondo fixed point on intermediate energy scales, $T_h \ll E \ll T_K$, with T_K in Eq. (2). Dimensional scaling yields the Zeeman scale

$$T_h = T_K (\bar{h}/T_K)^{M/2}, \quad \bar{h} = \max |h_{jk}|. \quad (5)$$

On energy scales below T_h , the Zeeman field drives the system away from the Kondo fixed point and nonperturbative methods are needed.

Charge transport.—The currents I_j flowing through the j th lead and the respective chemical potentials μ_j define the conductance tensor $G_{jk} = -e \frac{\partial I_j}{\partial \mu_k}$. Using the above bosonization approach, perturbation theory in the Zeeman field yields the linear conductances for $T_h \ll T \ll T_K$,

$$\begin{aligned} \frac{G_{jk}}{2e^2/h} &= Q_{jk} - \frac{\sin(2\pi/M)}{M} \left(\frac{T_h}{T} \right)^{4/M} \sum_{l \neq m} \frac{h_{lm}^2}{h^2} \quad (6) \\ &\times (Q_{jl} + Q_{jm})(Q_{lk} + Q_{mk}) + O(h_{jk}^4), \end{aligned}$$

with $Q_{jk} = \mathbf{w}_j \cdot \mathbf{w}_k = \delta_{jk} - 1/M$. It is instructive to analyze the diagonal term, G_{jj} , for just one non-zero Zeeman component, say h_{12} . Taking $j \neq 1, 2$, such that γ_j is not Zeeman-coupled to other Majoranas, Eq. (6) predicts a *reduction* with respect to the $h_{12} = 0$ result, $G_{jj} = \frac{2e^2}{h} \frac{M-1}{M}$. This reduction can be intuitively understood by noting that for $T \ll T_h$, the Zeeman field effectively removes the two Majoranas γ_1 and γ_2 from the low-energy sector, and thereby drives the system to a new fixed point with $M \rightarrow M - 2$. For $T \ll T_h$ (and $M > 4$), the conductance should therefore approach the *smaller* value $G_{jj} = \frac{2e^2}{h} \frac{M-3}{M-2}$. This scenario has also been found by exact Bethe ansatz calculations [38]. The temperature dependence of the above conductance coefficient is illustrated in Fig. 2.

Multi-point correlations.—Let us now address the correlation functions of the Majorana spin components at the Kondo fixed point. Two-point correlations are always diagonal and given by $\langle \mathcal{T}_\tau \mathcal{S}_{jk}^{(+)}(\tau) \mathcal{S}_{jk}^{(+)}(0) \rangle \simeq |T_K \tau|^{-2+4/M}$, where \mathcal{T}_τ denotes imaginary time ordering. In fact, this correlator directly implies Eq. (6) for the conductance tensor. However, the Majorana spin also exhibits remarkable multi-point correlations. For

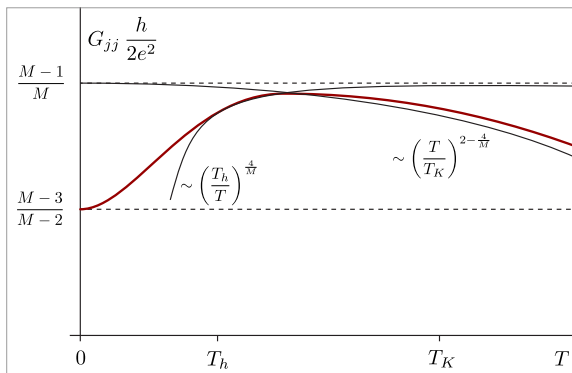


Figure 2. (Color online) Schematic sketch of the temperature (T) dependence of the linear conductance coefficient G_{jj} , with $j \neq 1, 2$, for $M > 4$ and a Zeeman field with $h_{12} \neq 0$. For $T \ll T_h$, the conductance approaches $\frac{2e^2}{h} \frac{M-3}{M-2}$, as appropriate for the $\text{SO}(M-2)$ fixed point. For $T_h \ll T \ll T_K$, on the other hand, it is the $\text{SO}(M)$ fixed point that governs the conductance, with $G_{jj} \simeq \frac{2e^2}{h} \left(\frac{M-1}{M} - c_1(T_h/T)^{4/M} - c_2(T/T_K)^{2-4/M} \right)$, where $c_{1,2}$ is of order unity.

clarity, we first consider the case $M = 3$, where the three Majorana spin components define a vector with $S_j = \sum_{kl} \varepsilon_{jkl} S_{kl}^{(+)}$. Within a Coulomb gas interpretation for the bosonized expression of the S_j , see Eq. (4), “neutral” phase combinations are required for the existence of multi-point correlators [39]. This leads to the three-point correlator,

$$\langle \mathcal{T}_\tau [S_j(\tau_1) S_k(\tau_2) S_l(\tau_3)] \rangle \simeq \frac{\varepsilon_{jkl}}{T_K (\tau_{12} \tau_{13} \tau_{23})^{1/3}}, \quad (7)$$

where $\tau_{jk} = \tau_j - \tau_k$ with all $T_K |\tau_{jk}| \gg 1$, and $\tau^{1/3} = \text{sgn}(\tau) |\tau|^{1/3}$. Equation (7) is consistent with the $\text{SO}(3)$ group structure and BCFT fusion rules [5, 28], and has observable consequences in the “spin response” to the Zeeman field vector \mathbf{h} with $h_j = \sum_{kl} \varepsilon_{jkl} h_{kl}$. In fact, perturbation theory in \mathbf{h} entails from Eq. (7) the effective action contribution

$$S_{\text{eff}} \sim \int dt_1 dt_2 dt_3 \frac{\mathbf{h}(t_1) \cdot [\mathbf{h}(t_2) \times \mathbf{h}(t_3)]}{T_K (t_{12} t_{13} t_{23})^{1/3}}, \quad (8)$$

where we switch to real time, $\tau \rightarrow it$, and allow for a time-dependent Zeeman field. Taking $\mathbf{h}(t) = (h_1 \cos[\omega_1 t], h_2 \cos[\omega_2 t], 0)$, the action (8) implies nonlinear frequency mixing, i.e., a finite magnetization $\langle S_3(t) \rangle$ that oscillates in time with frequencies $\omega_1 \pm \omega_2$. Similarly, for $\mathbf{h}(t) = (0, 0, h_3 \cos[\omega t])$ with $\omega \gg T_h$, the above action predicts that an oscillatory “transverse” spin correlation function is generated ($t_1 > t_2$),

$$\langle S_1(t_1) S_2(t_2) \rangle \sim h_3 \cos[\omega(t_1 + t_2)] F[\omega(t_1 - t_2)], \quad (9)$$

$$F(y) = (y/2)^{-1/6} [Y_{-1/6}(y) + J_{1/6}(y)],$$

with the Bessel functions Y_ν and J_ν . Since $F(y \gg 1) \simeq y^{-2/3} \cos(y - \pi/3)$, the envelope of the oscillatory correlations in Eq. (9) has the slow algebraic long-time tail

$\sim (t_1 - t_2)^{-2/3}$. Finally, we note that similar multi-point correlations appear also for $M > 3$. For odd M , the Coulomb gas neutrality condition allows for M -point correlations, while the $M/2$ -point correlator may survive for even M [37].

Experiment.—How can the above predictions be tested experimentally? Our predictions for the conductance should be readily observable in charge transport once the Kondo regime $T \ll T_K$ has been reached; similar experiments (but away from the Kondo regime) have been carried out previously [18, 20, 22]. While the observation of the magnetization components is less straightforward, the presence of definite multi-point correlations (7) makes them particularly interesting observables. For a single nanowire with $M = 2$ Majoranas, several readout schemes have been proposed before in the context of topological quantum computing [14–16, 40], by employing, e.g., a nearby quantum dot [17] or a flux qubit [41]. Building on these ideas, we here propose to probe the “magnetization”, $\sim i \langle \gamma_j \gamma_k \rangle$, via the occupation of the qubit state associated to the non-local fermion $c = (\gamma_j + i\gamma_k)/2$. The readout of this state might proceed in three steps: (i) Switch off all Zeeman couplings and decouple all leads, e.g., by ramping up gates indicated by vertical bars in Fig. 1, and reduce the charging gap of the island, e.g., by the gate voltage. (ii) Tunnel couple the end states j, k to a single-electron box. (iii) The occupation of the c fermion state may now be probed [17] by detecting the charge state of the single-electron box as function of its charging energy and of a magnetic flux threading the system, see Fig. 1.

To conclude, we have studied the dynamics of the effective quantum impurity spin formed by the spatially separated Majorana fermions in a topological Kondo device as shown in Fig. 1. This highly unconventional spin exhibits rich and observable dynamics characterized by nonvanishing multi-point correlations and nonperturbative crossovers between different non-Fermi liquid Kondo fixed points. We hope that the effects predicted here can soon be observed experimentally.

We thank E. Eriksson, A.A. Nersisyan, V. Kravtsov, and A. Zazunov for valuable discussions, and acknowledge financial support by the SFB TR12 and the SPP 1666 of the DFG, a Royal Society URF, and the DOE under Contract No. DE-AC02-98CH10886.

-
- [1] P. Nozières and A. Blandin, *J. Phys.* **41**, 193 (1980).
 - [2] A.M. Tselvick and P.B. Wiegmann, *Z. Phys. B* **54**, 201 (1984); *J. Stat. Phys.* **38**, 125 (1985).
 - [3] N. Andrei and C. Destri, *Phys. Rev. Lett.* **52**, 364 (1984).
 - [4] A.M. Tselvick, *J. Phys. C* **18**, 159 (1985).
 - [5] I. Affleck, *Nucl. Phys. B* **336**, 517 (1990); I. Affleck and A.W.W. Ludwig, *Nucl. Phys. B* **352**, 849 (1991); *ibid.* **360**, 641 (1991); *ibid.* **428**, 545 (1994).

- [6] A.O. Gogolin, A.A. Nersesyan, and A.M. Tsvelik, *Bosonization and strongly correlated systems* (Cambridge University Press, 1998).
- [7] A.C. Hewson, *The Kondo Problem to Heavy Fermions* (Cambridge University Press, 2008).
- [8] R.M. Potok, I.G. Rau, H. Shtrikman, Y. Oreg, and D. Goldhaber-Gordon, *Nature* **446**, 167 (2007).
- [9] B. Béri and N.R. Cooper, *Phys. Rev. Lett.* **109**, 156803 (2012).
- [10] S.R. Plissard, I. van Weperen, D. Car, M.A. Verheijen, G.W.G. Immink, J. Kammhuber, L.J. Cornelissen, D.B. Szombati, A. Geresdi, S.M. Frolov, L.P. Kouwenhoven, and E.P.A.M. Bakkers, *Nat. Nanotech.* **8**, 859 (2013).
- [11] A. Altland and R. Egger, *Phys. Rev. Lett.* **110**, 196401 (2013).
- [12] B. Béri, *Phys. Rev. Lett.* **110**, 216803 (2013).
- [13] A. Zazunov, A. Altland, and R. Egger, *New J. Phys.* **16**, 015010 (2014).
- [14] J. Alicea, *Rep. Prog. Phys.* **75**, 076501 (2012).
- [15] M. Leijnse and K. Flensberg, *Semicond. Sci. Techn.* **27**, 124003 (2012).
- [16] C.W.J. Beenakker, *Annu. Rev. Condens. Matter Phys.* **4**, 113 (2013).
- [17] K. Flensberg, *Phys. Rev. Lett.* **106**, 090503 (2011).
- [18] V. Mourik, K. Zuo, S.M. Frolov, S.R. Plissard, E.P.A.M. Bakkers, and L.P. Kouwenhoven, *Science* **336**, 1003 (2012).
- [19] L. Rokhinson, X. Liu, and J. Furdyna, *Nat. Phys.* **8**, 795 (2012).
- [20] A. Das, Y. Ronen, Y. Most, Y. Oreg, M. Heiblum, and H. Shtrikman, *Nat. Phys.* **8**, 887 (2012).
- [21] M.T. Deng, C.L. Yu, G.Y. Huang, M. Larsson, P. Caroff, and H.Q. Xu, *Nano Lett.* **12**, 6414 (2012).
- [22] H.O.H. Churchill, V. Fatemi, K. Grove-Rasmussen, M.T. Deng, P. Caroff, H.Q. Xu, and C.M. Marcus, *Phys. Rev. B* **87** 241401(R) (2013).
- [23] E.J.H. Lee, X.C. Jiang, M. Houzet, R. Aguado, C.M. Lieber, and S. De Franceschi, *Nature Nanotech.* **267**, 79 (2014).
- [24] A. Golub, I. Kuzmenko, and Y. Avishai, *Phys. Rev. Lett.* **107**, 176802 (2011).
- [25] I. Kuzmenko, A. Golub, and Y. Avishai, *Phys. Rev. B* **85**, 205313 (2012).
- [26] We assume that the energies of quasiparticle states besides the Majorana end states to be higher than the Kondo temperature. On general grounds, one expects the quasiparticle energies to be comparable to the proximity gap amplitude which, likewise, represents a high energy scale in our approach.
- [27] G.A. Fiete, W. Bishara, and C. Nayak, *Phys. Rev. Lett.* **101**, 176801 (2008); *Phys. Rev. B* **82**, 035301 (2010).
- [28] P. Di Francesco, P. Mathieu, and D. Sénéchal, *Conformal Field Theory* (Springer Verlag, New York, 1997).
- [29] J. von Delft and H. Schoeller, *Ann. Phys. (Berlin)* **7**, 225 (1998).
- [30] C. Nayak, M.P.A. Fisher, A.W.W. Ludwig, and H.H. Lin, *Phys. Rev. B* **59**, 15694 (1999).
- [31] M. Oshikawa, C. Chamon, and I. Affleck, *J. Stat. Mech. Theor. Exp.* **2006**, P02008 (2006).
- [32] L. Fu, *Phys. Rev. Lett.* **104**, 056402 (2010).
- [33] A. Zazunov, P. Sodano, and R. Egger, *New J. Phys.* **15**, 035033 (2013).
- [34] J. Lee and F. Wilczek, *Phys. Rev. Lett.* **111**, 226402 (2013).
- [35] H. Yi and C.L. Kane, *Phys. Rev. B* **57**, R5579 (1998).
- [36] H. Yi, *Phys. Rev. B* **65**, 195101 (2002).
- [37] See the accompanying Supplementary Material for additional information.
- [38] A. Altland, B. Béri, R. Egger, and A.M. Tsvelik, *J. Phys. A: Math. Theor.* **47**, 265001 (2014).
- [39] Note that a “bare” SO(3) Majorana spin also has three-point correlations. However, these do not depend on the $|\tau_{jk}|$ and do not cause the effects discussed here.
- [40] F.J. Burnell, A. Shnirman, and Y. Oreg, *Phys. Rev. B* **88**, 224507 (2013).
- [41] F. Hassler, A.R. Akhmerov, C.-Y. Hou, and C.W.J. Beenakker, *New J. Phys.* **12**, 125002 (2010).